

The Utility of Native MS for Understanding the Mechanism of Action of Repurposed Therapeutics in COVID-19: Heparin as a Disruptor of the SARS-CoV-2 Interaction with Its Host Cell Receptor

Yang Yang, Yi Du, and Igor A. Kaltashov*

Cite This: <https://dx.doi.org/10.1021/acs.analchem.0c02449>

Read Online

ACCESS |



Metrics & More

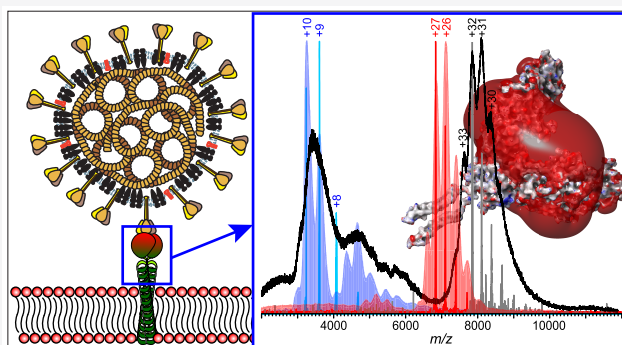


Article Recommendations



Supporting Information

ABSTRACT: The emergence and rapid proliferation of the novel coronavirus (SARS-CoV-2) resulted in a global pandemic, with over 6,000,000 cases and nearly 400,000 deaths reported worldwide by the end of May 2020. A rush to find a cure prompted re-evaluation of a range of existing therapeutics vis-à-vis their potential role in treating COVID-19, placing a premium on analytical tools capable of supporting such efforts. Native mass spectrometry (MS) has long been a tool of choice in supporting the mechanistic studies of drug/therapeutic target interactions, but its applications remain limited in the cases that involve systems with a high level of structural heterogeneity. Both SARS-CoV-2 spike protein (S-protein), a critical element of the viral entry to the host cell, and ACE2, its docking site on the host cell surface, are extensively glycosylated, making them challenging targets for native MS. However, supplementing native MS with a gas-phase ion manipulation technique (limited charge reduction) allows meaningful information to be obtained on the noncovalent complexes formed by ACE2 and the receptor-binding domain (RBD) of the S-protein. Using this technique in combination with molecular modeling also allows the role of heparin in destabilizing the ACE2/RBD association to be studied, providing critical information for understanding the molecular mechanism of its interference with the virus docking to the host cell receptor. Both short (pentasaccharide) and relatively long (eicosasaccharide) heparin oligomers form 1:1 complexes with RBD, indicating the presence of a single binding site. This association alters the protein conformation (to maximize the contiguous patch of the positive charge on the RBD surface), resulting in a notable decrease in its ability to associate with ACE2. The destabilizing effect of heparin is more pronounced in the case of the longer chains due to the electrostatic repulsion between the low-pI ACE2 and the heparin segments not accommodated on the RBD surface. In addition to providing important mechanistic information on attenuation of the ACE2/RBD association by heparin, the study demonstrates the yet untapped potential of native MS coupled to gas-phase ion chemistry as a means of facilitating rational repurposing of the existing medicines for treating COVID-19.



The emergence of the novel coronavirus (SARS-CoV-2) in late 2019¹ resulted in a global pandemic that had left virtually no country in the world unaffected.² The new disease (termed COVID-19) claimed over 400,000 lives worldwide by the end of May 2020, with the number of new cases still averaging over 100,000 daily in early June. This global crisis has resulted in a rush to find effective treatments for COVID-19, with strategies relying on repurposing of the existing medicines given high priority.³ While the initial efforts were largely empirical,^{4,5} the rapid progress in understanding the etiology of COVID-19 and accumulation of the vast body of knowledge on the SARS-CoV-2 life cycle and its mechanism of infectivity provided an extensive list of therapeutic targets for rational intervention.⁶ One such high-value target is the viral spike protein (S-protein),⁷ which is critical for both docking of the viral particle to its host cell surface receptor ACE2,⁸ and

the concomitant fusion with the cell membrane followed by the delivery of the viral load.⁹

One particularly promising avenue for therapeutic intervention that currently enjoys considerable attention is blocking the ACE2/S-protein interaction site with either antibodies or small molecules.¹⁰ In particular, heparin interaction with the S-protein has been shown to induce conformational changes within the latter¹¹ and to have inhibitory effects on the cellular entry by the virus.¹² Combined with the well-documented anticoagulant and anti-inflammatory¹³ properties of heparin

Received: June 8, 2020

Accepted: July 17, 2020

Published: July 17, 2020

(that are highly relevant vis-à-vis the two hallmarks of COVID-19, the coagulopathy^{14,15} and the cytokine storm¹⁶), this led to a suggestion that heparin or related compounds may play multiple roles in both arresting the SARS-CoV-2 infection and mitigating its consequences.^{17,18} In fact, heparin treatment of COVID-19 patients has been adopted by some physicians and is associated with a better prognosis.¹⁹ At the same time, the use of heparin raises the specter of heparin-induced thrombocytopenia (HIT), and its incidence was found to be particularly high among critical COVID-19 patients.²⁰ Clearly, utilization of heparin or related compounds as a safe and efficient treatment of coronavirus-related pathologies will hinge upon the ability to select a subset of structures that exhibit the desired properties (e.g., the ability to block the ACE2/S-protein association) while lacking the deleterious effects (e.g., the ability to create immunogenic ultralarge complexes with platelet factor 4, the hallmark of HIT,²¹ or cause excessive bleeding). Similar sentiments can be expressed with respect to a wide range of other medicines that are currently a focus of extensive repurposing efforts.³ This work can be greatly facilitated by analytical methods capable of providing detailed information on the drug candidates' interactions with their therapeutic targets and their ability to disrupt the molecular processes that are critical for the SARS-CoV-2 lifecycle. Native mass spectrometry (MS) has been steadily gaining popularity in the field of drug discovery,^{22,23} but its applications are frequently limited to relatively homogeneous systems. Unfortunately, the large size and the extensive glycosylation of the proteins involved in the SARS-CoV-2 docking to the host cell surface (14 N-glycans within the ectodomain of ACE2 and at least 18 O- and N-glycans within the S-protein ectodomain,²⁴ including three in its receptor binding domain, RBD) make the straightforward application of native MS to study ACE2/S-protein association challenging. This problem may be further exacerbated by the structural heterogeneity of therapeutics that are evaluated as potential disruptors of the ACE2/S-protein association, such as heparin and its derivatives.

Several approaches have been developed in the past decade as a means of facilitating native MS analyses of highly heterogeneous systems, which rely on supplementing MS measurements with nondenaturing front-end separation techniques,²⁵ and gas-phase chemistry (e.g., limited charge reduction²⁶). The latter is particularly attractive, as it allows native MS to be applied to systems as heterogeneous as associations of proteins with unfractionated heparin.²⁷ In this work, we use native MS in tandem with limited charge reduction to characterize ACE2/RBD complexes and evaluate the influence of heparin-related compounds (a synthetic pentasaccharide fondaparinux and a fixed-length eicosasaccharide heparin chains) on the stability of these complexes. Above and beyond providing important mechanistic details on attenuation of the ACE2/RBD association by heparin, the study demonstrates the potential of native MS supplemented by limited charge reduction to support the COVID-19-related drug repurposing efforts.

EXPERIMENTAL SECTION

The recombinant forms of human ACE2 (residues 1–740) and RBD (residues 319–541) expressed in baculovirus/insect cells systems were purchased from Sino Biological (Wayne, PA). RBD expressed in *E. coli* was purchased from RayBiotech (Peachtree Corners, GA). All proteins were extensively

dialyzed in 150 mM NH₄CH₃CO₂ prior to MS analyses (ultrafiltration at 2000 rpm with 10 kDa MW cutoff filters for 60 min repeated three times), although only proteins expressed in eukaryotic cells could be recovered following purification. Fondaparinux was purchased from Sigma-Aldrich (St. Louis, MO), and heparin eicosasaccharide produced by partial heparin depolymerization (dp20) was purchased from Iduron (Alderley Edge, UK). All solvents and buffers were of analytical grade or higher. Native MS measurements were carried out using a Synapt G2-Si (Waters, Milford, MA) hybrid quadrupole/time-of-flight mass spectrometer equipped with a nano-spray ion source. The following ion source parameters were used to maintain noncovalent complexes in the gas phase: capillary voltage, 1.5 kV; sampling cone voltage, 80 V; source offset, 80 V; trap CE, 4 V; trap DC bias, 3 V; and transfer CE, 0 V. Ion selection for limited charge reduction was achieved by setting the appropriate quadrupole selection parameters (LM resolution set at 4.5). Limited charge reduction was initiated by allowing the *m/z*-selected multiply charged ions to interact with 1,3-dicyanobenzene anions for 0.6 ms after setting the trap wave height as 0.3 V and optimizing the discharge current. All MS measurements were repeated at least twice to ensure consistency of the results.

Molecular modeling of the RBD/heparin complexes was carried out using a Maestro (Schrödinger LLC, New York, NY) modeling suite, release 2019-4. The ACE2/RBD model was prepared using the PDB 6M17 structure²⁸ as a template. The pentasaccharide model was extracted from the PDB 4R9W structure, and dp20 model was created by deleting a tetrasaccharide from the nonreducing end of heparin dp24 (PDB 3IRJ). The RBD/heparinoid complexes were minimized using the OPLS3 force field. The MD simulations were set up using a neutralized system (with 6 and 34 Na⁺ ions used for fondaparinux and dp20, respectively) and run for 6 ns in explicit water and 150 mM NaCl at 300 K under an OPLS3 force field.

RESULTS AND DISCUSSION

Despite the modest size of the SARS-CoV-2 receptor binding domain (RBD), its mass spectrum acquired under near-native conditions (Figure 1A) is convoluted and difficult to interpret. Since the main source of structural heterogeneity within this protein is its extensive glycosylation (two N- and at least one O-glycans²⁴), we also attempted to work with RBD expressed in *E. coli* (presumably glycan free). However, this construct had poor solubility characteristics and appeared to exist as a large aggregate, most likely due to the aberrant disulfide formation (see Supporting Information for more details). Therefore, our efforts were focused on using limited charge reduction²⁶ to facilitate the native MS analysis of this glycoprotein expressed in eukaryotic cells. Selection of a subpopulation of RBD ions at *m/z* 3256 (the apex of the most abundant peak) followed by their reaction with 1,3-dicyanobenzene anions over a limited period of time results in a reduction of the extent of multiple charging of RBD ions without fragmentation. As a result, a well-defined charge ladder is generated that allows both *z* and *m* values of the selected ionic population to be determined (the cyan trace in Figure 1A). This procedure allowed the major ionic species (*m/z* 2990–4100) to be assigned as the RBD monomers (average MW 32.7 kDa). Similar analysis of the minor ionic species (*m/z* 4200–6500) led to their assignment as the RBD dimers with an average MW 65.5 kDa (the blue trace in Figure 1A). The

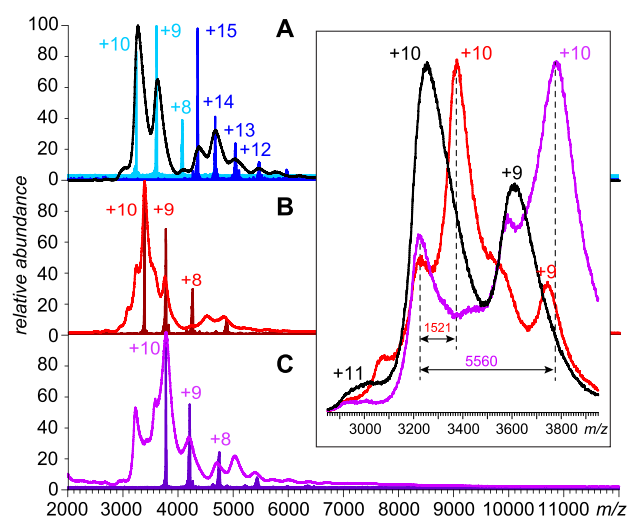


Figure 1. Mass spectra of the recombinant form of the SARS-CoV-2 S-protein RBD (10 μM aqueous solution in 150 mM $\text{NH}_4\text{CH}_3\text{CO}_2$) in the absence of heparinoids (A) and in the presence of 15 μM fondaparinux (B) and 15 μM fixed-length heparin oligomer dp20 (C). The charge states of the poorly defined peaks in the original mass spectra were assigned using limited charge reduction of ionic populations at m/z 3256 (cyan), 3375 (maroon), 3779 (purple), and 4358 (blue). The inset shows a zoomed view of the ionic signals at the charge state +10 in all three mass spectra.

latter likely reflects the presence of an unpaired cysteine residue within the RBD segment (Cys⁵³⁸) capable of forming an intermolecular disulfide bond.

Addition of a structurally homogeneous pentasaccharide heparin mimetic (fondaparinux) to the RBD solution results in a noticeable shift of the ionic signal in native MS (Figure 1B). The magnitude of this shift (1521 Da) correlates with the ligand mass (1505 Da); importantly, only 1:1 protein/ligand complexes are observed (in contrast to high-pI proteins, which act as heparin “sponges” by accommodating multiple polyanionic chains²⁹). Similar behavior is observed when a fixed-length heparin oligomer (eicosasaccharide, or dp20) is added to the RBD solution (Figure 1C). The magnitude of the mass shift (5.6 kDa) corresponds to a dp20 species carrying on average 26 sulfate groups (the sulfation levels in dp20 range from 17 to 28³⁰), and only 1:1 RBD/dp20 complexes are observed alongside the less abundant free protein (inset in Figure 1).

The absence of the 1:2 protein/heparin oligomer complexes might seem surprising, as the protein surface contains two distinct basic patches (R346, R355, K356, and R357) and (R454, R457, K458, K462, and R466) that were previously suggested to be heparin binding sites.¹¹ Molecular dynamics (MD) simulations of the RBD/fondaparinux complex indicates that the polyanion association with the protein results in significant conformational changes on the surface of the latter, giving rise to a consolidated patch of the positive charge (Figure 2). While such conformational rearrangements provide enthalpic gains for the electrostatically driven RBD/heparin oligomer interaction, they exert deleterious effects on the ACE2/RBD binding. Indeed, conformation of the receptor-binding motif (RBM) of RBD following RBD association with fondaparinux undergoes significant changes, which affect critical residues in the ACE2/RBD interface⁷ (see Supporting Information for more details).

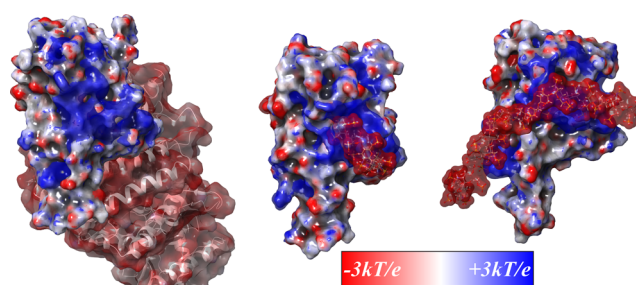


Figure 2. $3kT/e$ electrostatic potential (ESP) surfaces calculated for RBD associated with ACE2 (left), fondaparinux (middle), and dp20 (right). The ACE2/RBD structure (part of PDB 6M17²⁸) shows ACE2 in a ribbon format with an ESP-mapped molecular surface. Both RBD/heparinoid complexes are representative structures from MD simulations; the heparinoids are shown in a ball-and-stick format with ESP-mapped molecular surfaces.

To confirm the ability of a short heparin oligomer to disrupt the ACE2/RBD association, mass spectra of the ACE2/RBD mixture were acquired in the absence and in the presence of fondaparinux under near-native conditions. Native MS of ACE2 indicates that this protein is a noncovalent dimer (ACE₂, see Supporting Information for more details), and the reference ACE2/RBD spectrum (Figure 3A) features an

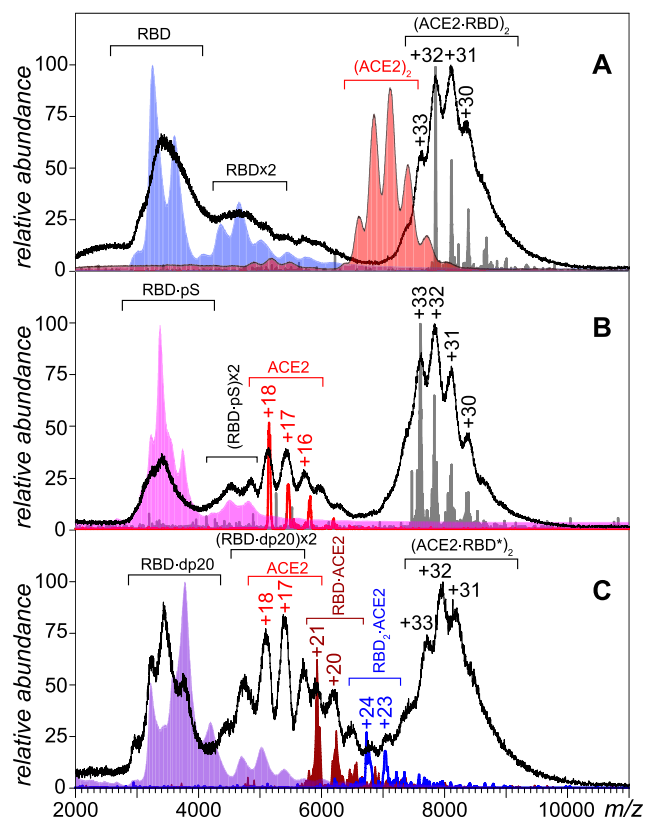


Figure 3. Mass spectra of RBD/ACE2 solutions (5 and 2.5 μM , respectively) in 150 mM $\text{NH}_4\text{CH}_3\text{CO}_2$ acquired in the absence of heparinoids (A) and in the presence of fondaparinux (B) and dp20 (C). The reference mass spectrum of ACE2 is shown in panel A (red); the blue, pink, and purple reference spectra in panels A, B, and C, respectively, represent RBD, RBD/fondaparinux, and RBD/dp20. The well-defined charge ladders in each panel show the results of the limited charge reduction measurements that were used to assign the poorly defined ion peaks in the original mass spectra.

abundant signal of the (ACE2·RBD)₂ complex in *m/z* region 7500–9000 (the mass and charge assignments for these ions were made using limited charge reduction in a manner similar to that described earlier for the RBD and its complexes with heparinoids) alongside the residual unbound RBD that was present in molar excess in solution. This is consistent with the crystal structure of the ACE2/RBD complexes, where each monomeric unit within the (ACE2)₂ dimer accommodates a single RBD molecule.^{28,31} No signal of unbound ACE2 could be detected, consistent with the reported binding strength in the low-nM range⁷ (total concentrations of both proteins in solutions used in MS analyses were in the low- μ M range (Figure 3). The appearance of the mass spectrum changes dramatically in the presence of fondaparinux (5-fold molar excess over RBD), with the ionic signal of ACE2 monomers becoming prominent in the *m/z* region 5000–6000 (Figure 3B). The presence of both free RBD and ACE2 species alongside their complex suggests a dramatic decrease in the binding affinity (which can be roughly estimated using the solution concentrations of both binding partners,³² i.e., in the μ M range). The destabilizing effect exerted by the longer heparinoid is even more significant. Indeed, the presence of dp20 in solution resulted in the ionic signals of free RBD and the ACE2 monomer becoming nearly equiabundant with that of their 2:2 complex; the spectrum also reveals the presence of monomeric ACE2 associated with the RBD dimer (Figure 3C).

The importance of the heparin oligomer chain length in modulating its ability to disrupt the ACE2/RBD interaction is likely to be related to the limited physical size of the positive patch on the RBD surface that can accommodate not more than six saccharide units (Figure 2). The rest of the polyanionic chain is exposed to the solvent, resulting in unfavorable interactions with the low-pI ACE2 molecules (due to the electrostatic repulsion). This results in a synergistic effect, with the longer heparin chain destabilizing the ACE2/RBD association via both conformational rearrangements within the former (vide supra) and the long-range electrostatic repulsion of the latter. It should also be noted that the ionic signal of the (ACE2·RBD)₂ complex in the presence of dp20 appears to have a mass shift in excess of 3 kDa compared to the same complex observed in the absence of heparin oligomers. It is possible that this mass shift reflects the presence of a lower-sulfate density heparin oligomer chain associated with the ACE2-bound RBD, with the low number of negative charges present on this glycosaminoglycan chain being insufficient *vis-à-vis* inducing unfavorable electrostatic interaction with the negatively charged ACE2. In contrast to the long and highly sulfated heparin chains, the shorter oligomer (fondaparinux) disrupts the ACE2/RBD interaction only via allosteric conformational changes within the RBM segment within RBD, exerting a somewhat weaker destabilizing effect. Taken together, the results of native MS measurements and MD simulations provide important insights into the mechanism of the ACE2/RBD association disruption by heparin that will be invaluable for rational selection of the most potent inhibitors of the SARS-CoV-2 docking to the host cell.

CONCLUSIONS

The level of structural heterogeneity displayed by both viral proteins and their counterparts on the surfaces of the host cells (as well as some of the proposed therapeutics, such as heparin) may seem overwhelming for the straightforward “intact-

molecule” MS measurements. However, incorporation of the limited charge reduction in the experimental workflow allows meaningful information to be obtained on objects as complex as 2:2 ACE2/RBD associations. While native MS cannot provide the level of structural detail produced in crystallographic studies,^{28,31} it allows the influence of various compounds on the stability of such complexes to be readily evaluated and mechanistic details to be revealed, thereby enabling a rational approach to the drug repurposing efforts. While the methodology presented in this work allows the overall effect of highly heterogeneous heparin products on the ACE2/RBD association to be determined, complementary MS-based methods of heparin analysis (such as the recently introduced foot-printing³⁰) will enable elucidation of specific structural features of heparin that endow it with high RBD affinity and/or enhanced ability to disrupt the ACE2/RBD associations. Design of successful therapeutic strategies against a foe as formidable as SARS-CoV-2 will require mobilization of efforts and resources in the entire field of life sciences, and analytical tools (including MS) will undoubtedly play a pivotal role in this work.

ASSOCIATED CONTENT

Supporting Information

The Supporting Information is available free of charge at <https://pubs.acs.org/doi/10.1021/acs.analchem.0c02449>.

ACE2 and RBD amino acid sequences, MS of *E. coli*-expressed RBD, MS and limited charge reduction analysis of ACE2, and details of MD studies of the heparin oligomers interactions with RBD (PDF)

AUTHOR INFORMATION

Corresponding Author

Igor A. Kaltashov – Department of Chemistry, University of Massachusetts-Amherst, Amherst, Massachusetts 01003, United States; orcid.org/0000-0002-4355-6039; Phone: (413) 545-1460; Email: kaltashov@chem.umass.edu

Authors

Yang Yang – Department of Chemistry, University of Massachusetts-Amherst, Amherst, Massachusetts 01003, United States

Yi Du – Department of Chemistry, University of Massachusetts-Amherst, Amherst, Massachusetts 01003, United States

Complete contact information is available at:

<https://pubs.acs.org/10.1021/acs.analchem.0c02449>

Author Contributions

Y.Y. designed and carried out the experimental work and analyzed the data. Y.D. carried out the molecular modeling work. I.A.K. designed the study, analyzed the data, and drafted the manuscript. All authors have given approval to the final version of the manuscript.

Notes

The authors declare no competing financial interest.

ACKNOWLEDGMENTS

This work was supported by grants from the National Institutes of Health (R01 GM112666) and the National Science Foundation (CHE-1709552). MS instrumentation used in this work is part of the Mass Spectrometry Core Facility at UMass-Amherst.

REFERENCES

- (1) Zhu, N.; Zhang, D.; Wang, W.; Li, X.; Yang, B.; Song, J.; Zhao, X.; Huang, B.; Shi, W.; Lu, R.; Niu, P.; Zhan, F.; Ma, X.; Wang, D.; Xu, W.; Wu, G.; Gao, G. F.; Tan, W. *N. Engl. J. Med.* **2020**, *382*, 727–733.
- (2) Freed, J. S.; Kwon, S. Y.; Jacobs El, H.; Gottlieb, M.; Roth, R. *Ann. Glob. Health* **2020**, *86*, 51.
- (3) Li, G.; De Clercq, E. *Nat. Rev. Drug Discovery* **2020**, *19*, 149–150.
- (4) Menzella, F.; Biava, M.; Barbieri, C.; Livrieri, F.; Facciolo, N. *Drugs in Context* **2020**, *9*, 2020–2024 2026.
- (5) Shin, H.-S. *Infect. Chemother.* **2020**, *52*, No. 217.
- (6) Zhou, H.; Fang, Y.; Xu, T.; Ni, W. J.; Shen, A. Z.; Meng, X. M. *Br. J. Pharmacol.* **2020**, *177*, 3147–3161.
- (7) Walls, A. C.; Park, Y.-J.; Tortorici, M. A.; Wall, A.; McGuire, A. T.; Velesler, D. *Cell* **2020**, *181*, 281–292.
- (8) Wan, Y.; Shang, J.; Graham, R.; Baric, R. S.; Li, F. *J. Virol.* **2020**, *94*, No. e00127-20.
- (9) Tang, T.; Bidon, M.; Jaimes, J. A.; Whittaker, G. R.; Daniel, S. *Antiviral Res.* **2020**, *178*, 104792.
- (10) Zhang, H.; Penninger, J. M.; Li, Y.; Zhong, N.; Slutsky, A. S. *Intensive Care Med.* **2020**, *46*, 586–590.
- (11) Mycroft-West, C.; Su, D.; Elli, S.; Li, Y.; Guimond, S.; Miller, G.; Turnbull, J.; Yates, E.; Guerrini, M.; Fernig, D.; Lima, M.; Skidmore, M. The 2019 coronavirus (SARS-CoV-2) surface protein (Spike) S1 Receptor Binding Domain undergoes conformational change upon heparin binding. *bioRxiv*, 2020. DOI: 10.1101/2020.02.29.971093.
- (12) Mycroft-West, C. J.; Su, D.; Pagani, I.; Rudd, T. R.; Elli, S.; Guimond, S. E.; Miller, G.; Meneghetti, M. C. Z.; Nader, H. B.; Li, Y.; Nunes, Q. M.; Procter, P.; Mancini, N.; Clementi, M.; Forsyth, N. R.; Turnbull, J. E.; Guerrini, M.; Fernig, D. G.; Vicenzi, E.; Yates, E. A., et al. Heparin inhibits cellular invasion by SARS-CoV-2: structural dependence of the interaction of the surface protein (spike) S1 receptor binding domain with heparin. *bioRxiv*, 2020. DOI: 10.1101/2020.04.28.066761.
- (13) Young, E. *Thromb. Res.* **2008**, *122*, 743–752.
- (14) Helms, J.; Tacquard, C.; Severac, F.; Leonard-Lorant, I.; Ohana, M.; Delabranche, X.; Merdji, H.; Clere-Jehl, R.; Schenck, M.; Fagot Gandet, F.; Fafi-Kremer, S.; Castelain, V.; Schneider, F.; Grunebaum, L.; Angles-Cano, E.; Sattler, L.; Mertes, P. M.; Meziani, F. *Intensive Care Med.* **2020**, *46*, 1089–1098.
- (15) Giannis, D.; Ziogas, I. A.; Gianni, P. *J. Clin. Virol.* **2020**, *127*, 104362.
- (16) Mehta, P.; McAuley, D. F.; Brown, M.; Sanchez, E.; Tattersall, R. S.; Manson, J. J. *Lancet* **2020**, *395*, 1033–1034.
- (17) Thachil, J. *J. Thromb. Haemostasis* **2020**, *18*, 1020–1022.
- (18) Lindahl, U.; Li, J. P. *J. Thromb. Haemostasis* **2020**, na DOI: 10.1111/jth.14898.
- (19) Tang, N.; Bai, H.; Chen, X.; Gong, J.; Li, D.; Sun, Z. *J. Thromb. Haemostasis* **2020**, *18*, 1094–1099.
- (20) Liu, X.; Zhang, X.; Xiao, Y.; Gao, T.; Wang, G.; Wang, Z.; Zhang, Z.; Hu, Y.; Dong, Q.; Zhao, S.; Yu, L.; Zhang, S.; Li, H.; Li, K.; Chen, W.; Bian, X.; Mao, Q.; Cao, C. Heparin-induced thrombocytopenia is associated with a high risk of mortality in critical COVID-19 patients receiving heparin-involved treatment. *medRxiv*, 2020. DOI: 10.1101/2020.04.23.20076851.
- (21) Rauova, L.; Poncz, M.; McKenzie, S. E.; Reilly, M. P.; Arepally, G.; Weisel, J. W.; Nagaswami, C.; Cines, D. B.; Sachais, B. S. *Blood* **2005**, *105*, 131–138.
- (22) Hannah, V. V.; Atmanene, C.; Zeyer, D.; Van Dorsselaer, A.; Sanglier-Cianferani, S. *Future Med. Chem.* **2010**, *2*, 35–50.
- (23) Tong, W.; Wang, G. *Methods (Amsterdam, Neth.)* **2018**, *144*, 3–13.
- (24) Shajahan, A.; Supekar, N. T.; Gleinich, A. S.; Azadi, P. *Glycobiology* **2020**, na DOI: 10.1093/glycob/cwaa042.
- (25) Kaltashov, I. A.; Pawlowski, J. W.; Yang, W.; Muneeruddin, K.; Yao, H.; Bobst, C. E.; Lipatnikov, A. N. *Methods (Amsterdam, Neth.)* **2018**, *144*, 14–26.
- (26) Abzalimov, R. R.; Kaltashov, I. A. *Anal. Chem.* **2010**, *82*, 7523–7526.
- (27) Zhao, Y.; Abzalimov, R. R.; Kaltashov, I. A. *Anal. Chem.* **2016**, *88*, 1711–1718.
- (28) Yan, R.; Zhang, Y.; Li, Y.; Xia, L.; Guo, Y.; Zhou, Q. *Science (Washington, DC, U. S.)* **2020**, *367*, 1444–1448.
- (29) Niu, C.; Yang, Y.; Huynh, A.; Nazy, I.; Kaltashov, I. A. *Biophys. J.* **2020**, na DOI: 10.1016/j.bpj.2020.04.012.
- (30) Niu, C.; Zhao, Y.; Bobst, C. E.; Savinov, S. N.; Kaltashov, I. A. *Anal. Chem.* **2020**, *92*, 7565–7573.
- (31) Lan, J.; Ge, J.; Yu, J.; Shan, S.; Zhou, H.; Fan, S.; Zhang, Q.; Shi, X.; Wang, Q.; Zhang, L.; Wang, X. *Nature* **2020**, *581*, 215–220.
- (32) Leverence, R.; Mason, A. B.; Kaltashov, I. A. *Proc. Natl. Acad. Sci. U. S. A.* **2010**, *107*, 8123–8128.